FEA-Assisted Steady-State Modelling of a Spoke Type IPM Machine with Enhanced Flux Weakening Capability

Nada Elloumi Ahmed Masmoudi
University of Sfax
Research Laboratory on Renewable Energies and Electric Vehicles (RELEV), Sfax 3072, Tunisia,
Email:
elloumi.nada@gmail.com, a.masmoudi@enis.rnu.tn

Mauro Bortolozzi Alberto Tessarolo
University of Trieste
Engineering and Architecture Department, 34127 Trieste, Italy
Email:
mauro.bortolozzi@gmail.com atessarolo@units.it

***Abstract*—Interior permanent magnet (IPM) machines with spoke-type design are possible candidates for various applications, including vehicle traction. One of their drawback is the high demagnetizing current required in the flux weakening region to let the motor achieve high speeds. This problem can be mitigated by equipping the motor with a mechanical devices consisting of mobile rotor yokes. These move radially by centrifugal force so as to reduce the air-gap flux at high speed with no need for demagnetizing current injection. This paper addresses the problem of modeling such IPM motor to study its steady-state behavior under different operating conditions, both in the full-flux and in the flux-weakening region of the speed range. The approach uses a limited set of non-linear finite element analysis to characterize the dependency of motor flux linkages on the stator currents and rotor position. Interpolating functions are then obtained to mathematically capture this dependency and plug it into the steady-state electromechanical equations of the motor. The effectiveness and accuracy of the method are assessed through on-load measurements taken on the modelled motor both in low and high speed operation.**

Keywords— Permanent magnet machines; finite element analysis; steady state analytical model;

I. Introduction

Spoke-type internal permanent magnet (IPM) machines are an attractive architecture for automotive, household and industrial applications due to their high efficiency, high torque density and absence of excitation field windings. As already known, one of the major drawbacks of permanent magnet motors is the difficulty of reducing the excitation flux to extend the speed range of the machine. Generally, the flux weakening is performed injecting a demagnetizing current along the *d*-axis [1]-[3]. This approach is known to have several disadvantages, one of them is the efficiency reduction due to copper loss increase. In order to mitigate the impact of the flux weakening on the machine performance, there are several techniques in the literature proposing alternative mechanical methods to reduce the magnet excitation flux during high speed operating conditions [4]-[8].

In this paper, an automatic mechanical rotor flux weakening device is considered. This device, proposed in [8], consists of a ferromagnetic back iron retained by some springs. The device is designed to activate (so as to reduce the magnet flux) automatically due to centrifugal force when the speed exceeds a given threshold that can be decided in the design stage.

In order to predict the machine behavior at any load

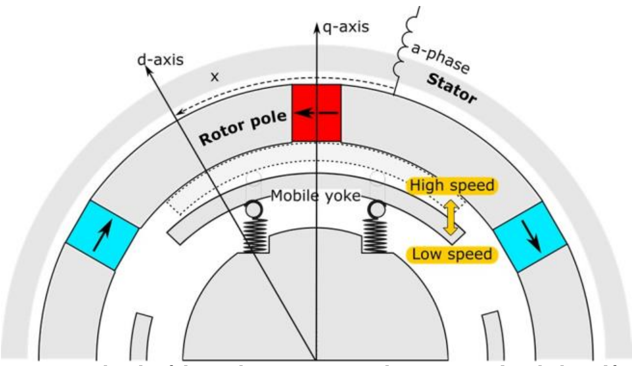

Figure 1. Sketch of the spoke type IPM machine equipped with the self-activated flux weakening device.

condition, an accurate and reliable mathematical model is required. The aim of this work is to build a simple steady state electro-mechanical model for this kind of IPM machine based on *d* and *q* flux linkage determination through finite element analysis (FEA). For the sake of simplicity only two mechanical cases are considered. The “high speed case” with the yokes attached to the rotor structure and the “low speed case” with the yokes detached (Figure 1).

The proposed methodology is based on the determination of the *d* and *q* flux linkages as a function of the *d* and *q* currents respectively. This occurrence is possible as far as we neglect the inductance cross-coupling effect.

After obtaining a database of the of the *d* and *q* fluxes as a function of the *d* and *q* currents (using FEA), an interpolation function is used to obtain the corresponding “flux map”.

These “flux maps” are obtained for both detached and attached yoke cases. As a further step, the flux maps are incorporated into the classical *d-q* steady state IPM machine model. This mathematical model allows to determine the machine steady state behavior at any defined working point condition.

The of approach can be considered as innovative because there are no examples in the literature so far about this kind of machines modeled with an analytical FEA-assisted technique. The obtained model is finally assessed using experimental measurements performed on a custom-made test bench and a good accordance is found between experimental and theoretical results.

The paper is organized as follows: Section II is about the electro-mechanical IPM machine model description; Section III described the flux map determination; finally, there the mathematical model solution is discussed along with the experimental validation.

II. MATEMATICAL MODEL FOR A PM MACHINE

The relationship between voltages, currents and fluxes, for a generic three phase synchronous machine, is represented by the well-known expression:

$$v_{abc} = R_s\, i_{abc} + \frac{d(\$_{abc}(x))}{dt} \quad (1)$$

where:

$$v_{abc} = \begin{bmatrix} v_a \\ v_b \\ v_c \end{bmatrix},\ i_{abc} = \begin{bmatrix} i_a \\ i_b \\ i_c \end{bmatrix},\ R_s = \begin{bmatrix} R & 0 & 0 \\ 0 & R & 0 \\ 0 & 0 & R \end{bmatrix} \text{ and}$$

$$\$_{abc}(x) = \$^s_{abc}(x) + \$^m_{abc}(x) = \begin{bmatrix} \$^c_a(x) \\ \$^c_b(x) \\ \$^c_c(x) \end{bmatrix} + \begin{bmatrix} \$^n_a(x) \\ \$^n_b(x) \\ \$^n_c(x) \end{bmatrix}. \quad (2)$$

$\$^s_{abc}(x)$ is the flux linkage vector due to the stator currents and $\$^m_{abc}(x)$ is the flux linkage vector due to the rotor field. Both these components are depending on the coordinate *x* (Figure 1).

All the electrical quantities in equation (1) are time dependent. In order to obtain a time-invariant mathematical model, it is necessary to introduce the power invariant Clarke-Park transformation. This transformation is represented by the following matrix (3):

$$T(x) = P(x) \cdot C \quad (3)$$

where:

$$C = \sqrt{\frac{2}{3}} \begin{bmatrix} 1 & -\frac{1}{2} & -\frac{1}{2} \\ 0 & \frac{\sqrt{3}}{2} & -\frac{\sqrt{3}}{2} \\ \frac{1}{\sqrt{2}} & \frac{1}{\sqrt{2}} & \frac{1}{\sqrt{2}} \end{bmatrix} \quad (4)$$

$$P(x) = \begin{bmatrix} \cos(x) & \sin(x) & 0 \\ -\sin(x) & \cos(x) & 0 \\ 0 & 0 & 1 \end{bmatrix}. \quad (5)$$

It is worth noticing that the matrix **T**(x) multiplied by its transpose is the identity matrix:

$$T(x) \cdot T(x)^u = I. \quad (6)$$

Therefore, assuming the *d*-axis aligned with the rotor pole symmetry axis (Figure 1) and considering the following definitions:

$$V_{dq} = T(x) \cdot v_{abc} = \begin{bmatrix} V_d \\ V_q \\ V_0 \end{bmatrix},$$
$$I_{dq} = T(x) \cdot i_{abc} = \begin{bmatrix} I_d \\ I_q \\ I_0 \end{bmatrix},$$
$$\$^c_{dq} = T(x) \cdot \$^c_{abc} = \begin{bmatrix} \Phi^c_d \\ \Phi^c_q \\ \Phi^c_0 \end{bmatrix}, \quad (7)$$
$$\$^n_{dq} = T(x) \cdot \$^n_{abc} = \begin{bmatrix} \Phi^h_d \\ 0 \\ 0 \end{bmatrix},$$

and:

$$R_{dq} = T(x) R_c T^u(x) = R_s \quad (8)$$

after some algebraic manipulations it is possible to rewrite the equation (1) in the *dq* reference frame as follows:

$$V_{dq} = R_s I_{dq} + mJ0^c_{dq} + \left(\frac{d0^c_{dq}}{dt}\right) + mJ0^m_{dq} \quad (9)$$

where:

$$J = \begin{pmatrix} 0 & -1 & 0 \\ 1 & 0 & 0 \\ 0 & 0 & 0 \end{pmatrix} \quad (10)$$

In case of steady state conditions, equation (9) becomes:

$$V_{dq} = R_s I_{dq} + mJ0^s_{dq} + mJ0^m_{dq}. \quad (11)$$

Now, neglecting omopolar components, the formula (11) can be can be replaced by a system of equations as follows:

$$\begin{cases} V_d = RI_d - mh_q \\ V_q = RI_q + mh_d \end{cases} \quad (12)$$

were:

$$h_d = \phi_d^c + \phi_d^n$$
$$h_q = \phi_q^c \tag{13}$$

h_d and h_q are the machine direct and quadrature flux linkages. Both these fluxes can be expressed as a function of stator currents I_d and I_q. This relationship is provided in the next section interpolating the results of some finite element simulations.

In a generic permanent magnet machine, the active electric power can be expressed as a function of the *d* and *q* currents and fluxes as follows:

$$P_e = V_d I_d + V_q I_q = $$
$$= R(I_d^2 + I_q^2) + mp(h_d I_q - h_q I_d) \tag{14}$$

The power-invariant Clarke-Parke transformation, represented by the matrix $\mathbf{T}(x)$, preserves the value of the active power. This said, using the system (12), the relationship between the phase voltage rms value and the *d*, *q* fluxes and currents is:

$$V_{rnc} = \sqrt{\frac{(RI_d - mh_q)^2 + (RI_q + mh_d)^2}{3}} \tag{15}$$

Thanks to (15), the general electro-mechanical model of the permanent magnet machine can be expressed as follows:

$$\begin{cases} 3V_{rnc}^2 = (RI_d - mh_q)^2 + (RI_q + mh_d)^2 \\ P_e = R(I_d^2 + I_q^2) + m(h_d I_q - h_q I_d) \end{cases} \tag{16}$$

III. DETERMINATION OF THE D AND Q FLUX LINKAGES FOR THE IPM MACHINE WITH MOBILE YOKES

In order to achieve a complete identification of the flux linkage of the machine, some FEA simulations are run for various values of I_d and I_q for both low and high speed conditions. From each simulation, the correspondent flux linkage is computed and stored. As already said before, this analysis is simplified by the fact that we can neglect the inductance cross coupling effect, so we can write:

$$h_d = h_d(I_d) = f(I_d)$$
and
$$h_q = h_q(I_q) = f'(I_q) \tag{17}$$

The flux database built with FEA simulations can be used to derive two different interpolating functions, (represented with *f* and *f'* in the expression ((17).

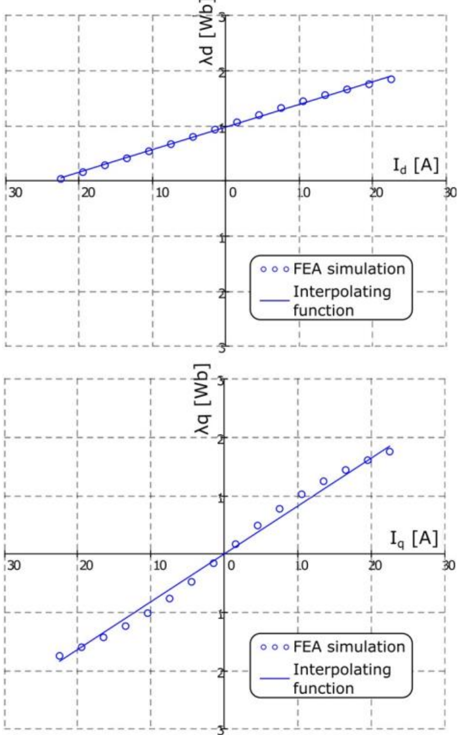

Figure 2. FEA-based computation of d-q phase flux linkages versus the armature current d-q components for the machine with detached yokes.

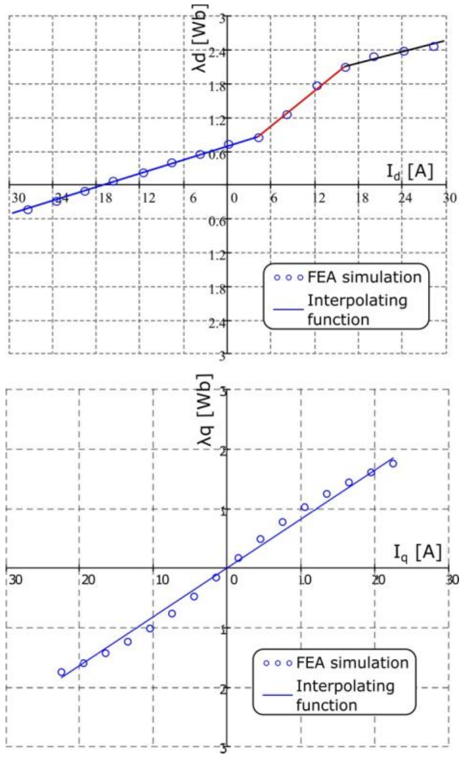

Figure 3: FEA-based computation of d-q phase flux linkages versus the armature current d-q components for the machine with attached yokes.

This identification has to be performed for both high and low speed conditions considered (Figure 5).

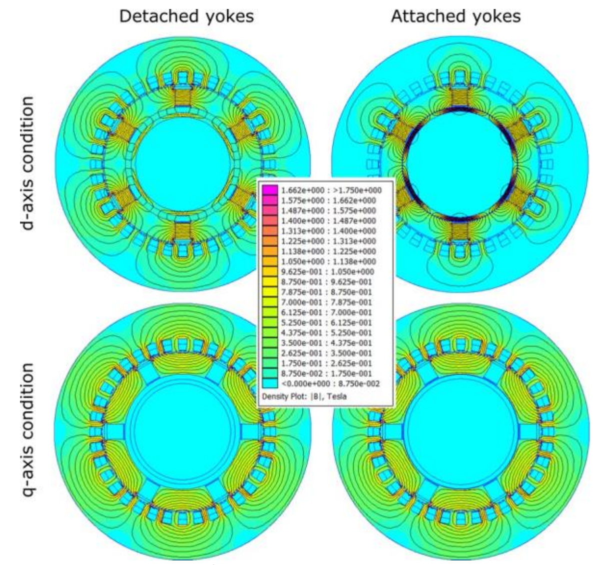

Figure 5. FEM model of the mobile yokes machine under d or q stator current. All the models have the same current amplitude.

A. Low speed case

The low speed case, also named detached-yokes case, is represented in Figure 5 on the left side. In this condition, all the mobile yokes are 5 millimeters distant from the inner surface of the rotor. The direct axis flux linkage database can be evaluated feeding the stator coils of the machine with a set of direct currents. In the same way, the quadrature flux linkages are calculated imposing a set of quadrature currents in the machine stator windings. All the magnetic core is considered non-linear. The functions fitting the original data are reported in (18). More in particular, the interpolating function for the direct flux in the low speed case is named $f^{LC}(I_d)$.

The comparison between the data derived from the simulation and the interpolating function is reported in Figure 2.

$$\begin{cases} f^{LC}(I_d) = h_d(I_d) = 0.992 + 0.044 I_d \\ f'(I_q) = h_q(I_q) = 0.11 I_q \end{cases} \quad (18)$$

B. High speed case

The high-speed case is represented in Figure 5 on the right side. In this condition all the mobile yokes are attached to the inner surface of the rotor. With the same approach used for the low speed case we can obtain the interpolating function for the attached yokes condition (19).

$$\begin{cases} f^{HC}(I_d) = h_d(I_d) = \begin{cases} 0.69 + 0.041 I_d & \text{if } -30 \le I_d \le 4 \\ 0.4 + 0.105 I_d & \text{if } 4 € I_d \le 16 \\ 1.51 + 0.035 I_d & \text{if } 16 € I_d \le 30 \end{cases} \\ f'(I_q) = h_q(I_q) = 0.11 I_q \end{cases} \quad (19)$$

The interpolating function for the direct flux in the high speed case is named $f^{HC}(I_d)$. It is worth noting that in this case it has been necessary to use a linear piecewise interpolating function defined for I_d that goes from -30 A to 30 A. The linear interpolation for the quadrature axis flux is the same as the one for the low speed case. This because the quadrature axis flux is not affected by the yoke position.

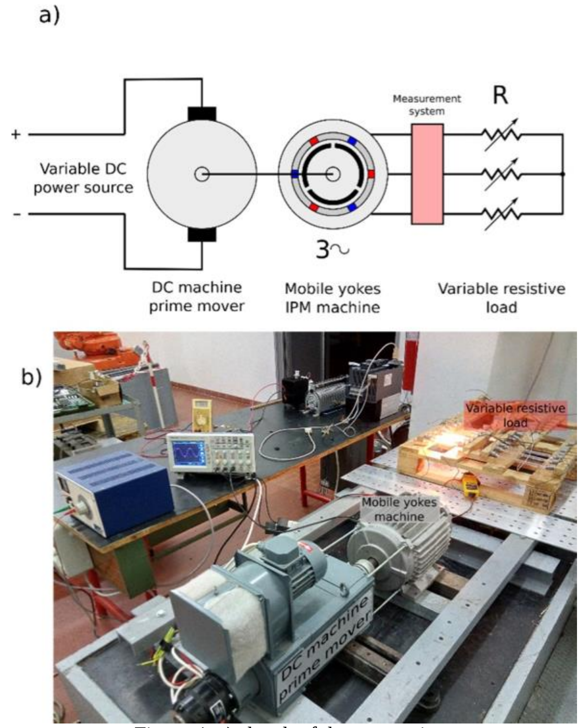

Figure 4: a) sketch of the connections
b) Test bench used for the experimental measurements.

IV. STEADY-STATE EQUATION SOLUTION AND EXPERIMENTAL VALIDATIONS

As already shown before the PM machine electro-mechanical model is a nonlinear set of equations. Substituting now the expression (18) into the system of equations (16), we obtain the final electro-mechanical model for the machine running at low speed (lower than the mobile- yoke activation threshold).

$$\begin{cases} 3V_{rnc}^2 = (RI_d - m f'(I_q))^2 + (RI_q + m f^{LC}(I_d))^2 \\ P_e = R(I_d^2 + I_q^2) + m(f^{LS}(I_d)I_q - f'(I_q)I_d) \end{cases} \quad (20)$$

On the other hand, the final electro-mechanical model for the machine running at high speed can be derived substituting (19) into (16):

$$\begin{cases} 3V_{rnc}^2 = (RI_d - m f'(I_q))^2 + (RI_q + m f^{HC}(I_d))^2 \\ P_e = R(I_d^2 + I_q^2) + m(f^{KS}(I_d)I_q - f'(I_q)I_d) \end{cases} \quad (21)$$

By solving these nonlinear systems imposing the voltage of the machine, it is possible to calculate the resultant currents (*d* and *q*) for a given power. The proposed approach has been assessed using experimental measurements on a custom-made test bench (Figure 4).

The system used for the measurements is composed of the PM synchronous machine under test connected to a variable speed DC prime mover. The mobile-yokes machine used as a generator is then connected to a variable resistive load (Figure 4). Two different cases have been investigated: one with the detached yokes (low speed), and one with attached yokes (speed higher than the mobile-yoke activation threshold).

The ratings of the tested machine are provided in Table 1.

TABLE 1: MACHINE UNDER TEST MAIN DATA

Rated phase voltage [V]	220
Rated current [A]	8
Number of poles	6
Phase resistance [Ω]	0.195
Base speed [rpm]	1000
Maximum speed [rpm]	2500
Mobile yokes activation threshold [rpm]	1200

In table 2 the measurements results are provided:

TABLE 2: MEASURED VALUES

	Low speed case	High speed case
Phase voltage [V_{rms}]	55	169
Phase current [A]	3.01	5.50
Active Power [W]	493	2793
Frequency [Hz]	15	75
Speed [rpm]	300	1500

Substituting the measured phase voltage and the measured power reported in Table 2 in the systems (20) and (21) we can calculate I_d and I_q and then the machine phase current:

TABLE 3: CALCULATED CURRENTS

	High speed case	Low speed case
I_d [A]	-8.34	-2.69
I_q [A]	4.685	4.43
I^{phace} [A_{rms}]	2.99	5.523

The machine phase current rms value can be evaluated as follows knowing the I_d and I_q currents:

$$I^{phace} = \sqrt{\frac{3}{2}}\left(\sqrt{I_d^2 + I_q^2}\right) \quad (22)$$

Looking at the table 3 it is worth notice that the calculated current I^{phace} for both the considered cases is almost equivalent to the current measured during the load test.

V. CONCLUSIONS

In conclusion, one can state that the proposed analytical FEA-assisted machine model is a good tool to predict the behavior of IPM motors equipped with a mechanical flux-weakening device of electrical machines in a generic steady-state operating condition. The main advantage of this kind of approach is the minimal amount of numerical computations required, the easy inclusion magnetic saturation non-linearity and the good accuracy in physical performance prediction.

REFERENCES

[1] S.-I. Kim, J. Cho, S. Park, T. Park, and S. Lim, *Characteristics comparison of a conventional and modified spoke-type ferrite magnet motor for traction drives of low-speed electric vehicles*, IEEE Trans. Ind. Appl., vol. 49, no. 6, pp. 2516–2523, Nov./Dec. 2013.

[2] J. Aubry, H. B. Ahmed, and B. Multon, *Sizing optimization methodology of a surface permanent magnet machine-converter system over a torque-speed operating profile: Application to a wave energy converter*, IEEE Trans. Ind. Electron., vol. 59, no. 5, pp. 2116–2125, May 2012.

[3] C. Jo, J.-Y. Seol, and I.-J. Ha, *Flux-weakening control of IPM motors with significant effect of magnetic saturation and stator resistance*, IEEE Trans. Ind. Electron., vol. 55, no. 3, pp. 1330–1340, Mar. 2008.

[4] R. Menis, M. Mezzarobba, and A. Tessarolo, *A survey of mechanical and electromagnetic design techniques for permanent-magnet motor flux-weakening enhancement*, in Proc. Elect. Syst. Aircraft, Railway, Ship Propuls. (ESARS), Oct. 2012, pp. 1–6

[5] H. Woehl-Bruhn, W.-R. Canders, and N. Domann, *Classification of field-weakening solutions and novel PM machine with adjustable excitation*, in Proc. 19th Int. Conf. Elect. Mach. (ICEM), Sep. 2010, pp. 1–6.

[6] K. Baoquan, L. Chunyan, and C. Shukang, *Flux-weakening characteristic analysis of a new permanent magnet synchronous motor used for electric vehicles*, IEEE Trans. Plasma Sci., vol. 39, no. 1, pp. 511–515, Jan. 2011.

[7] I. Boldea and L. N. Tutelea, *PMSM with rotor PM mechanical flux-weakening (MFW) to zero for an 150kW, 600Vdc, 500–6000 rpm drive: Preliminary design with key validation*, 2016 XXII International Conference on Electrical Machines *(ICEM)*, Lausanne, 2016, pp. 1995-2001.

[8] A. Tessarolo, M. Mezzarobba and R. Menis, *Modeling, Analysis, and Testing of a Novel Spoke-Type Interior Permanent Magnet Motor with Improved Flux Weakening Capability*, in IEEE Transactions on Magnetics, vol. 51, no. 4, pp. 1-10, April 2015.